




ORIGINAL RESEARCH

Circulating miR-19b-3p as a Novel Prognostic Biomarker for Acute Heart Failure

Yang Su , MD, PhD*; Yuxi Sun, MD*; Yansong Tang, MD; Hao Li, MD, PhD; Xiaoyu Wang, MD; Xin Pan, MD; Weijing Liu, MD, PhD; Xianling Zhang, MD, PhD; Fenglei Zhang, MD; Yawei Xu, MD, PhD; Chunxi Yan, MD; Sang-Bing Ong , PhD; Dachun Xu , MD, PhD

BACKGROUND: Circulating microRNAs are emerging biomarkers for heart failure (HF). Our study aimed to assess the prognostic value of microRNA signature that is differentially expressed in patients with acute HF.

METHODS AND RESULTS: Our study comprised a screening cohort of 15 patients with AHF and 5 controls, a PCR-discovery cohort of 50 patients with AHF and 26 controls and a validation cohort of 564 patients with AHF from registered study DRAGON-HF (Diagnostic, Risk Stratification and Prognostic Value of Novel Biomarkers in Patients With Heart Failure). Through screening by RNA-sequencing and verification by reverse-transcription quantitative polymerase chain reaction, 9 differentially expressed microRNAs were verified (miR-939-5p, miR-1908-5p, miR-7706, miR-101-3p, miR-144-3p, miR-4732-3p, miR-3615, miR-484 and miR-19b-3p). Among them, miR-19b-3p was identified as the microRNA signature with the highest fold-change of 8.4 and the strongest prognostic potential (area under curve with 95% CI, 0.791, 0.654–0.927). To further validate its prognostic value, in the validation cohort, the baseline level of miR-19b-3p was measured. During a follow-up period of 19.1 (17.7, 20.7) months, primary end point comprising of all-cause mortality or readmission due to HF occurred in 48.9% patients, while patients in the highest quartile of miR-19b-3p level presented the worst survival (Log-rank $P < 0.001$). Multivariate Cox model showed that the level of miR-19b-3p could independently predict the occurrence of primary end point (adjusted hazard ratio, 1.39; 95% CI, 1.18–1.64). In addition, miR-19b-3p positively correlated with soluble suppression of tumorigenicity 2 and echocardiographic indexes of left ventricular hypertrophy.

CONCLUSIONS: Circulating miR-19b-3p could be a valuable prognostic biomarker for AHF. In addition, a high level of circulating miR-19b-3p might indicate ventricular hypertrophy in AHF subjects.

REGISTRATION: URL: <https://www.clinicaltrials.gov>. Unique Identifier: NCT03727828.

Key Words: acute heart failure ■ biomarker ■ miR-19b-3p ■ prognosis ■ RNA-sequencing

Acute heart failure (AHF) is a severe cardiac syndrome that carries a high risk of hospital readmission and mortality. Predicting the outcome of patients with AHF has been a challenging task. Although various circulating peptides, such as natriuretic peptides, have been shown to facilitate the diagnosis and guidance of short and long term therapy in

patients with AHF their drawbacks limit their potential as prognostic biomarkers. Recently, microRNAs (miRNAs) have been gaining attention due to their promising role as potential biomarkers for stratifying patients with cardiac diseases.¹

miRNAs are small non-coding RNAs that orchestrate homeostasis through acting on post-transcription

Correspondence to: Dachun Xu, MD, PhD, Department of Cardiology, Shanghai Tenth People's Hospital, Tongji University School of Medicine, 315 Yanchang Middle Road, Shanghai, China. E-mail: xdc77@tongji.edu.cn

*Y. Su and Y. Sun contributed equally.

Supplementary Material for this article is available at <https://www.ahajournals.org/doi/suppl/10.1161/JAHA.121.022304>

For Sources of Funding and Disclosures, see page 11.

© 2021 The Authors. Published on behalf of the American Heart Association, Inc., by Wiley. This is an open access article under the terms of the Creative Commons Attribution-NonCommercial-NoDerivs License, which permits use and distribution in any medium, provided the original work is properly cited, the use is non-commercial and no modifications or adaptations are made.

JAHA is available at: www.ahajournals.org/journal/jaha

CLINICAL PERSPECTIVE

What Is New?

- miR-19b-3p is identified as a novel prognostic microRNA signature for acute heart failure population.
- The baseline level of miR-19b-3p was strongly correlated with echocardiographic indexes of left ventricular hypertrophy and the fibrosis-related biomarker soluble suppression of tumorigenicity 2.

What Are the Clinical Implications?

- The expression level of miR-19b-3p at the onset of acute heart failure could predict the prognosis and function as a potential biomarker for stratification of patients with acute heart failure.
- The association of miR-19b-3p with hypertrophic and fibrosis indexes prompts for further investigations to reveal the pathogenesis of acute heart failure.

Nonstandard Abbreviations and Acronyms

AHF	acute heart failure
HFpEF	heart failure with preserved ejection fraction
IVST	interventricular septal thickness
LVMI	left ventricular mass index
LVPWT	left ventricular posterior wall thickness
NYHA	New York Heart Association
sST2	soluble suppression of tumorigenicity 2

process. Due to their considerable stability, circulating miRNAs have been promoted as ideal biomarkers for heart failure (HF).^{2,3} Moreover, as miRNAs regulate various biophysiological processes, the presence of certain miRNAs can be harnessed to identify particular types of HF such as ischemic HF,^{4,5} systolic HF,⁶ HF with preserved ejection fraction (HFpEF),⁷ and HF due to dilated cardiomyopathy.⁸ Hence, miRNAs are promising indicators for the risk stratification and prognosis of HF.

In recent years, over ten miRNAs that play a diagnostic and prognostic role in AHF subjects have been identified,⁹ and some of them could indeed uncover the underlying mechanisms contributing to AHF. For instance, an aberrant miR-22 level could indicate the disturbance of calcium homeostasis and myofilament protein content under stress,¹⁰ and levels of miR-21 and miR-30a/b could indicate the severity of acute

kidney injury.^{11,12} Therefore, further investigations of miRNAs are warranted to unravel the mechanisms and optimize the management of HF.

The present study was aimed at exploring circulating miRNAs associated with AHF using RNA-sequencing and identifying the miRNA signature for prognosis. We then validate its prognostic potential in a prospective cohort incorporating 564 patients with AHF and investigate its clinical relevance with serological and echocardiographical measurements.

METHODS

The data that support the findings of this study are available from the corresponding author upon reasonable request.

Patient Recruitment

The study design is illustrated in Figure 1. Three independent cohorts were built for screening, PCR-discovery of miRNA candidates, and validation of the miRNA signature. (1) The screening cohort comprised 15 patients with AHF and 5 control subjects; (2) the PCR-discovery cohort comprised 50 patients with AHF and 26 control subjects; (3) the prospective validation cohort comprised 564 patients with AHF from registered DRAGON-HF (Diagnostic, Risk Stratification and Prognostic Value of Novel Biomarkers in Patients With Heart Failure) study (ClinicalTrials.gov, NCT03727828). The diagnosis of AHF was in accord with 2016 ESC Guidelines of HF, all patients were consecutively enrolled and received standard-of-care according to the guidelines.¹

Inclusion criteria for the validation cohort were as follows: (1) at least 18 years of age; (2) admission for diagnosed AHF (New York Heart Association [NYHA] classification from II to IV); (3) acquired consent form. Patients were excluded if complicated with one of the following: (1) acute myocardial infarction; (2) acute pulmonary embolism; (3) acute stroke; (4) preexisting organ failure (chronic cirrhosis, uremia, or end-stage cancer); (5) pregnancy.

This study complies with the Declaration of Helsinki, and has been approved by the local Ethics Committee. All participants have signed informed consent forms.

Data Collection

Demographic characteristics, medical history, and medication were determined at admission. Transthoracic echocardiography was performed by an experienced echocardiologist within 24 hours of admission. Echocardiographic parameters including left ventricular end-diastolic diameter (LVEDD), left ventricular end-systolic diameter (LVESD), interventricular septal thickness (IVST) and left ventricular posterior

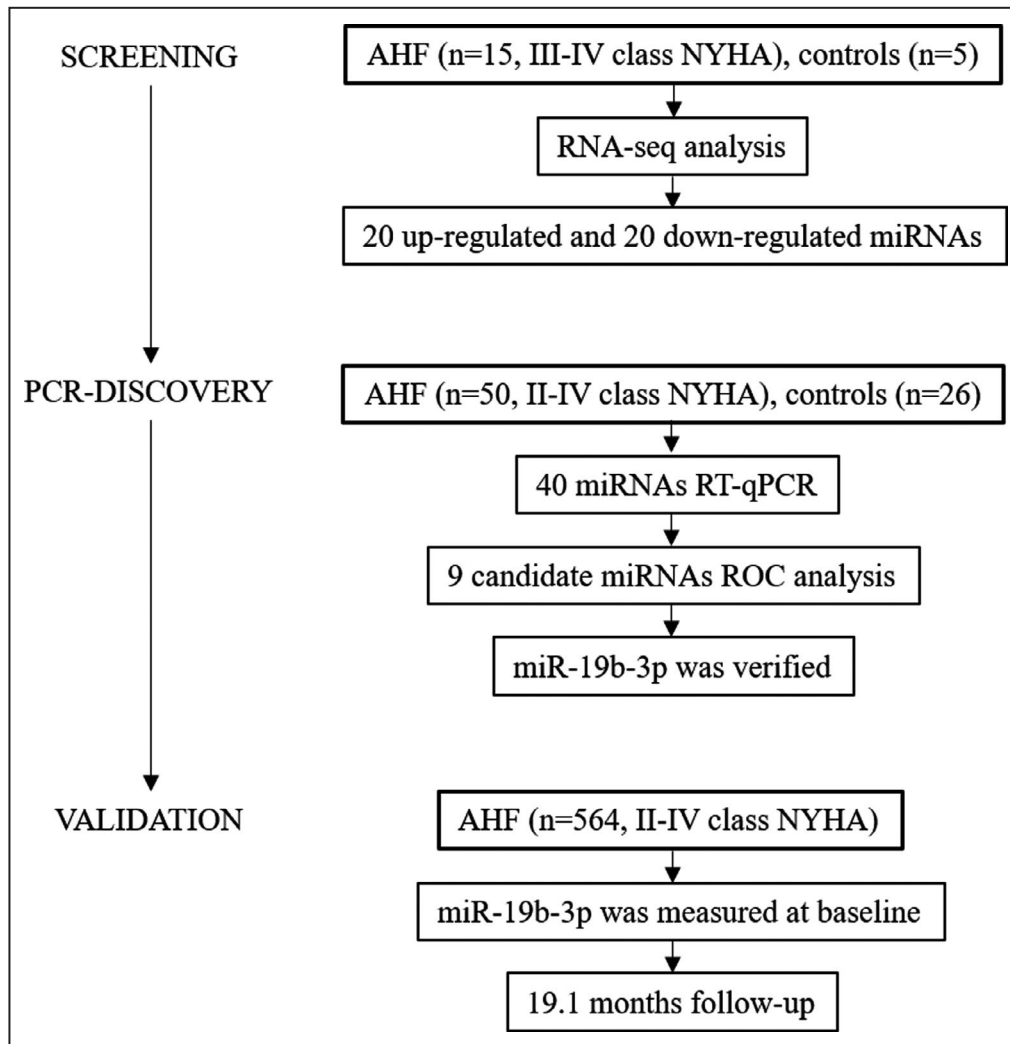


Figure 1. Flow chart of the study.

AHF indicates acute heart failure; NYHA, New York Heart Association; ROC, receiver operating characteristics; and RT-qPCR, Quantitative Real-time Polymerase Chain Reaction.

wall thickness (LVPWT) were measured by two experienced physicians using MyLab 30 CB machine (ESAOTE SPA) according to the recommendations of the American Society of Echocardiography and the European Association of Echocardiography.¹³ Left ventricular mass index (LVMI) was calculated by the formula: $LVMI (g/m^2) = (0.8 \times 1.04 \times ((LVEDD + LVPWT + IVST)^3 - (LVEDD)^3) + 0.6) / BSA$ (body surface area, m^2).

Subjects of PCR-discovery cohort were scheduled to have 1-year follow-up. And subjects of validation cohort underwent scheduled follow-up in the third, sixth, twelfth month, and every year since then. The primary end point was the composite of all-cause mortality and re-admission due to HF. At every scheduled follow-up or readmission, medical history and physical examination were taken by experienced physicians, and electrocardiography and blood samples were

collected. Other examinations were conducted as deemed necessary.

Serological Measurements

Baseline blood samples were obtained on admission prior to any treatment. Venous blood samples were collected for detection of soluble suppression of tumorigenicity 2 (sST2), NT-proBNP (N-terminal pro brain natriuretic peptide), and other biochemical indicators. NT-proBNP level was measured by an automated electrochemiluminescence immunoassay (Elecsys proBNP II assay). The remaining blood samples were centrifuged by two-step method (4 °C at 820×g for 10 minutes, then 4 °C at 16000×g for 10 minutes)¹⁴ and the supernatant was preserved at -80 °C with RNase/DNase-free tubes for further miRNAs and sST2 detection. sST2 levels were detected

using Human ST2/IL-33R Quantikine ELISA Kit (R&D Systems, Minneapolis, MN).¹⁵ The sST2 level of patients were calculated from the mean value of two repeated measurements of blood sample. Total RNAs were extracted from serum samples of screening cohort patients, and RNA-sequencing was performed to figure out differentially expressed miRNAs. Confirmation and validation of candidate miRNAs were accomplished by using real-time polymerase chain reaction (PCR) in PCR-discovery and validation cohort. (The description in details for miRNA profiling, PCR detection, primer sequences and bioinformatic analysis were showed in Data S1 and Table S1 with references [16–23] cited in the order as in the main manuscript).

Statistical Analysis

Bioinformatics Analysis of RNA-Sequencing Data

In the screening process, false discovery rate <0.01 and fold change >2 are taken as the screening criteria by default. In total, 20 up-regulated and 20 down-regulated miRNAs with the most significant difference (P value <0.05) in expression were selected. Based on GO and KEGG databases, the miRNAs involving in pathophysiological processes of cardiovascular diseases were selected for PCR verification. For miRNA verified in the PCR-discovery cohort, the diagnostic and prognostic power were assessed by receiver-operator characteristics (ROC) analysis. To better quantitatively identify the miRNA signature that has the highest diagnostic and prognostic power, the area under curve (AUC) was compared among candidates. Subsequently, the signature was adopted for further validation.

Clinical Data Analysis

Descriptive statistics were obtained for all study variables. Continuous data were expressed as mean±SD or median with interquartile range. Categorical data were expressed as proportions. All continuous variables were compared using the t-test or the Mann-Whitney U-test if appropriate. Categorical variables were analyzed for the study outcome by Fisher exact test or χ^2 test. Logarithmic transformation was applied for variables including NT-proBNP, sST2, and miRNAs in order to conform normal distribution. To validate the prognostic value of the signature and compare with other biomarkers, and further investigate the underlying association, survival analysis was adopted for validation.

The validation cohort was divided into four quartiles based on the baseline level of the miRNA signature. Clinical measurements were compared among four quartiles using analysis of variance if

data complied normal distribution with homogeneity of variance or sign rank test if not. The associations of miR-19b-3p with clinical measurements was analyzed by Pearson correlation and Spearman rank correlation analysis. The prognosis among four quartiles was assessed by survival analysis using Kaplan-Meier estimate and P -value was generated by Log-Rank test. Besides, univariate and multivariate Cox proportional hazard models were applied to evaluate the prognostic value, and the hazard ratio with corresponding 95% CI was calculated for investigating the risk factors of the primary end point. The multivariate model was adjusted for age, sex, body mass index, systolic blood pressure, NT-proBNP, atrial fibrillation history, coronary heart disease history, diabetes history, and estimated glomerular filtration rate.

Clinical data were analyzed using SPSS version 25.0 (IBM Corp) and Graphpad Prism 8.0.1 (GraphPad Software, San Diego, CA). For all the statistical analyses, 2-sided P <0.05 was considered significant.

RESULTS

miRNAs Expression Profile in the Screening Cohort

In the screening phase, demographic characteristics were almost similar between 15 patients with AHF and 5 controls. However, patients with AHF had distinctly higher NT-proBNP level (2521.0 versus 78.0 ng/L, P <0.001), worse cardiac function (left ventricular ejection fraction, 28.7±7.9% versus 65.4%±2.6%, P <0.001), worse renal function (estimated glomerular filtration rate 76.4±24.4 versus 107.7±22.5 mL/min×1.73 m², P =0.021), and lower high density lipoprotein levels (1.02±1.17 versus 1.71±0.33 mmol/L, P =0.004) (Table S2).

RNA-sequence analysis documented that a portion of miRNAs had a strong positive correlation between patients with AHF and controls (Figure S1A). As we displayed overall P -value (Figure S1B), 218 miRNAs were differentially expressed in patients with AHF. Eventually, 40 miRNA candidates (20 up-regulated and 20 down-regulated) with the highest fold-change were screened for validation (Figure S1C and S1D).

Verification of miRNA Expression and Identification of miRNA Signature

qPCR of the 40 selected miRNAs was undertaken with circulating RNA obtained from the PCR-discovery cohort composed of 50 patients with AHF and 26 health controls (Table S2). This cohort has an average age of 66.7±11.1 years old, and the proportion of

women was 69.3%. Among these, a total of 9 miRNAs (miR-939-5p, miR-1908-5p, miR-4732-3p, miR-7706, miR-3615, miR-484, miR-19b-3p, miR-101-3p, and miR-144-3p) were successfully validated and showed significantly different expression level (Figure 2). miR-19b-3p presented the highest level of up-regulation (fold change=8.4). ROC curve showed that all 9 validated miRNAs could discriminate patients with AHF from controls, and miR-19b-3p had the highest AUC value of 0.753 (Figure 3).

To preliminarily evaluate the prognostic potential of 9 miRNAs candidates, ROC analysis for the occurrence of end point events was performed (Figure 4). Three miRNAs showed significant *P*-value (miR-19b-3p, miR-484 and miR-3615), and miR-19b-3p presented the strongest power for discriminating patients with AHF who had occurrence of events from those had not. Therefore, miR-19b-3p was identified as the miRNA signature and underwent further validation.

Validation of miR-19b-3p in the Validation Cohort

The clinical significance of miR-19b-3p was further evaluated in the validation cohort. A total of 564 patients with AHF were divided into 4 quartiles according to the baseline level of miR-19b-3p. As shown in Table, the validation cohort was composed of more men (64.5%), and the median age was 69.0 [62.0, 77.0] years old. Demographic characteristics and medication at discharge (shown in Table S3) were similar among 4 groups.

In further investigating the clinical relevance of miR-19b-3p, we found significant positive correlations with serum sST2 ($r=0.583$) and echocardiographic indexes of left ventricular hypertrophy including IVST ($r=0.437$), LVPWT ($r=0.285$) and LVMI ($r=0.492$). However, no significant correlation was found between miR-19b-3p and NT-proBNP, left ventricular ejection fraction (Figure S2).

To validate the prognostic value of miR-19b-3p, occurrence of clinical events were compared among 4 quartiles of the cohort. Figure 5 shows the differences in occurrence of the primary end points (all cause-mortality or HF readmission) among patients in different quartiles of baseline miR-19b-3p levels. Through a follow-up period of 19.1 [17.7, 20.7] months, the event-free survival worsened from Q1 to Q4. A count of 83 out of 141 patients with AHF of Q4 reached primary end point, presenting the worst survival among 4 quartiles (Log-Rank $P<0.001$).

Subsequently, multivariate Cox proportional hazard model showed that baseline miR-19b-3p levels could predict the occurrence of the primary end points in overall population [hazard ratio, 1.39; 95% CI, 1.18–1.64] (Figure 6).

DISCUSSION

This is a large cohort study investigating the profiling of miRNA among 564 patients with AHF in China. The salient findings from this study include detection of miR-19b-3p as the most abundantly expressed miRNA among patients with AHF and the fact that miR-19b-3p achieved the highest prognostic value for primary cardiovascular events among patients with AHF. Furthermore, independent positive associations were found between circulating miR-19b-3p and serum sST2, LVMI, IVST and LVPWT in the AHF cohort, which implied a positive association between miR-19b-3p and ventricular hypertrophy.

In recent decades, multiple miRNAs have been identified as biomarkers for AHF diagnosis or prognosis. 5 up-regulated miRNAs, including miR-150-5p,²⁴ miR-1306-5p,²⁵ miR-92b-5p,²⁶ miR-302 family,²⁷ and miR-499,²⁸ and 7 down-regulated miRNAs, including miR-7i-5p, miR-18a-5p, miR-18b-5p, miR-223-3p, miR-301a-3p, miR-423-5p, and miR-652-3p⁹ have been previously identified. A growing number of miRNAs were found to play important roles in the pathogenesis of AHF, although not much is known about their association with different clinical features. In the present study, we identified the novel circulating miR-19b-3p that not only diagnose AHF, but also revealed its positive association with LV hypertrophy indices and cardiac fibrosis biomarker sST2. This suggests that an elevation of circulating miR-19b-3p could indicate fibrogenetic and hypertrophic responses in AHF subjects, which could exacerbate the condition of AHF.

miR-19b-3p belongs to the miRNA cluster miR-17-92, which is an important modulator in heart diseases.²⁹ In the in vitro studies, it had been illustrated that miR-19b-3p participated in the cardiac fibrosis process through modulating transforming growth factor-beta pathway and phosphatase and tensin homologue gene expression. Zou et al found that over-expressed miR-19a-3p/19b-3p in human cardiac fibroblasts could reduce transforming growth factor-beta signaling by targeting transforming growth factor-beta receptor II mRNA, and therefore inhibit autophagy-mediated fibrogenesis.³⁰ Another study by Zhong et al explored that over-expressed miR-19b-3p in rat cardiac fibroblast could promote proliferation and migration fibroblast by down-regulating phosphatase and tensin homologue expression.³¹ In the in vivo studies, Fang et al have demonstrated in humans that circulating miR-19b-3p could indicate diffused cardiac fibrosis - a pivotal pathophysiological alteration of HF,^{32,33} as confirmed by cardiac magnetic resonance.³⁴ In the present study, circulating miR-19b-3p was proposed to have a significant positive correlation with cardiac fibrosis biomarker sST2.³⁵ Moreover, we identified that circulating miR-19b-3p

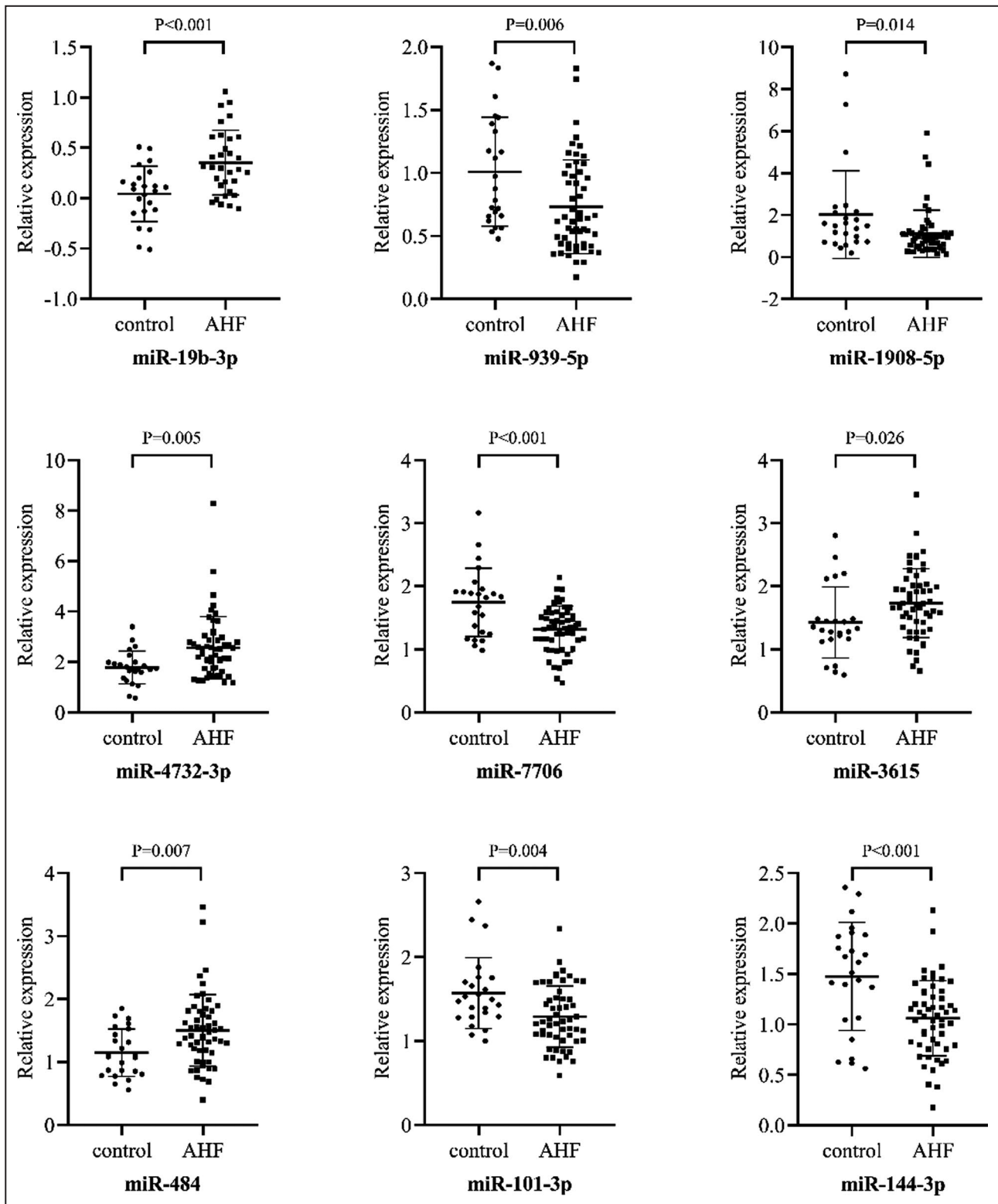


Figure 2. Relative expression of 9 verified miRNAs between patients with AHF and control.

miRNA candidates were verified in 50 AHFs and 26 controls by real-time quantitative polymerase chain reaction. Out of 40 candidates, 9 were verified with significant differential expression and miR-19b-3p presented the highest relative expression fold-change of 8.4. AHF indicates acute heart failure.

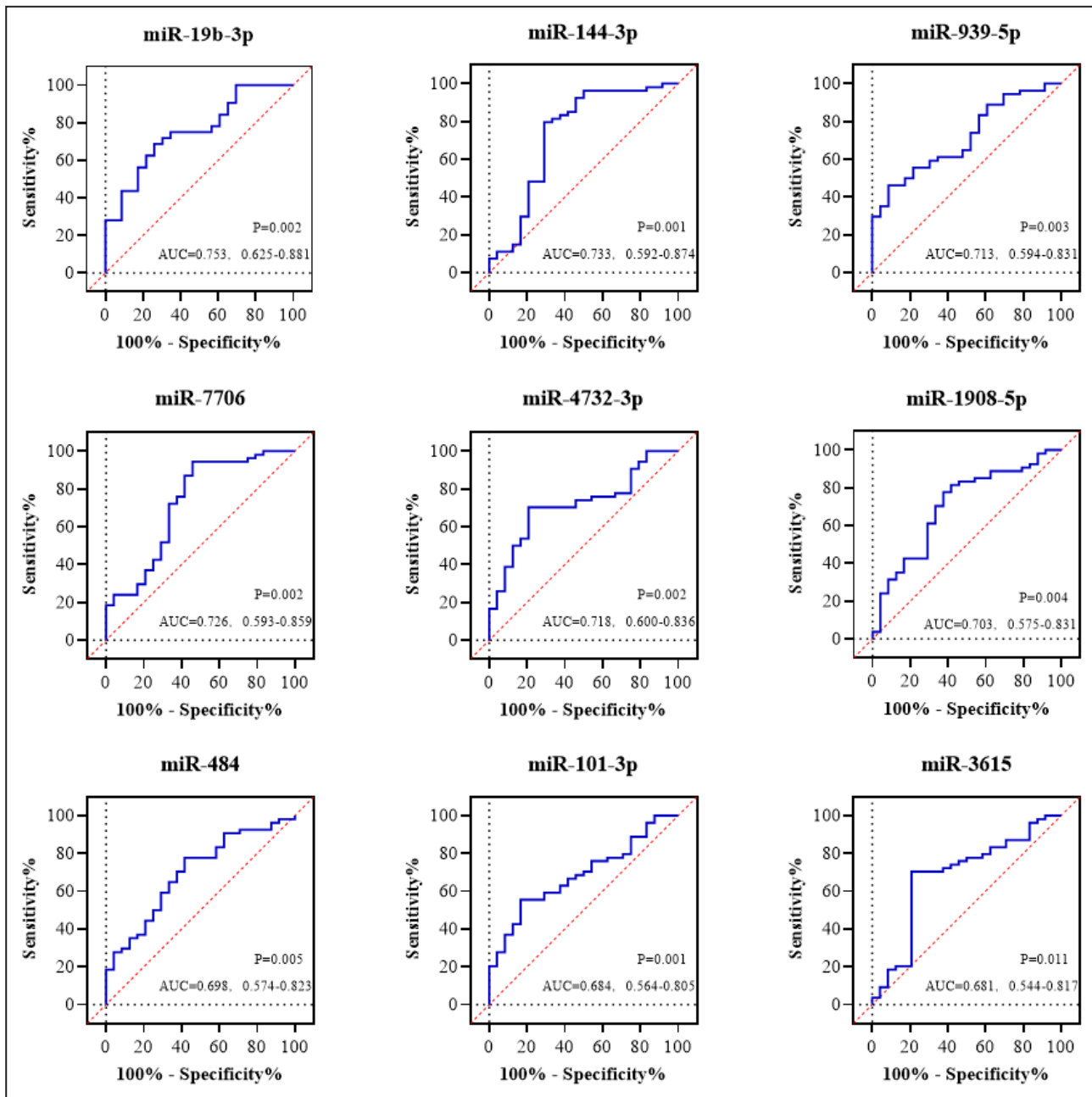


Figure 3. Receiver operating characteristic curves of 9 validated miRNAs for diagnosis of AHF.

Receiver operating characteristic curves were performed to test the diagnostic value of 9 miRNA candidates for AHF in PCR-discovery cohort. miR-19b-3p was found to have the highest discriminative potential for AHF (AUC=0.753). AHF denotes acute heart failure, AUC area under curve. Lower right annotation in each figure showed AUC with 95% CI and *P* value.

levels are positive related to LV hypertrophy indices. The enumerated researches on regulating role of miR-19b-3p about cardiac fibrosis provided solid evidences to support our finding mentioned above from a molecular biological perspective.

Besides fibrosis, miR-19b-3p modulates various pathophysiological processes that influence cardiac metabolism as demonstrated in the settings of diabetic cardiomyopathy,³⁶ vascular smooth muscle cell proliferation,³⁷ angiogenesis in endothelial cells

of coronary artery,³⁸ and inhibition of renal fibrosis.³⁹ Both endothelial dysfunction and RAAS activation by renal remodeling have been demonstrated to deteriorate cardiac failing. Moreover, our clinical evidence also indicates that miR-19b-3p predict worsened outcome of patients with AHF, where a higher level of circulating miR-19b-3p (divided by median value of 2.15) posed a 1.31-fold higher risk for mortality and HF readmission of patients with AHF. Integrating all available evidences, we believe that miR-19b-3p is a promising prognostic

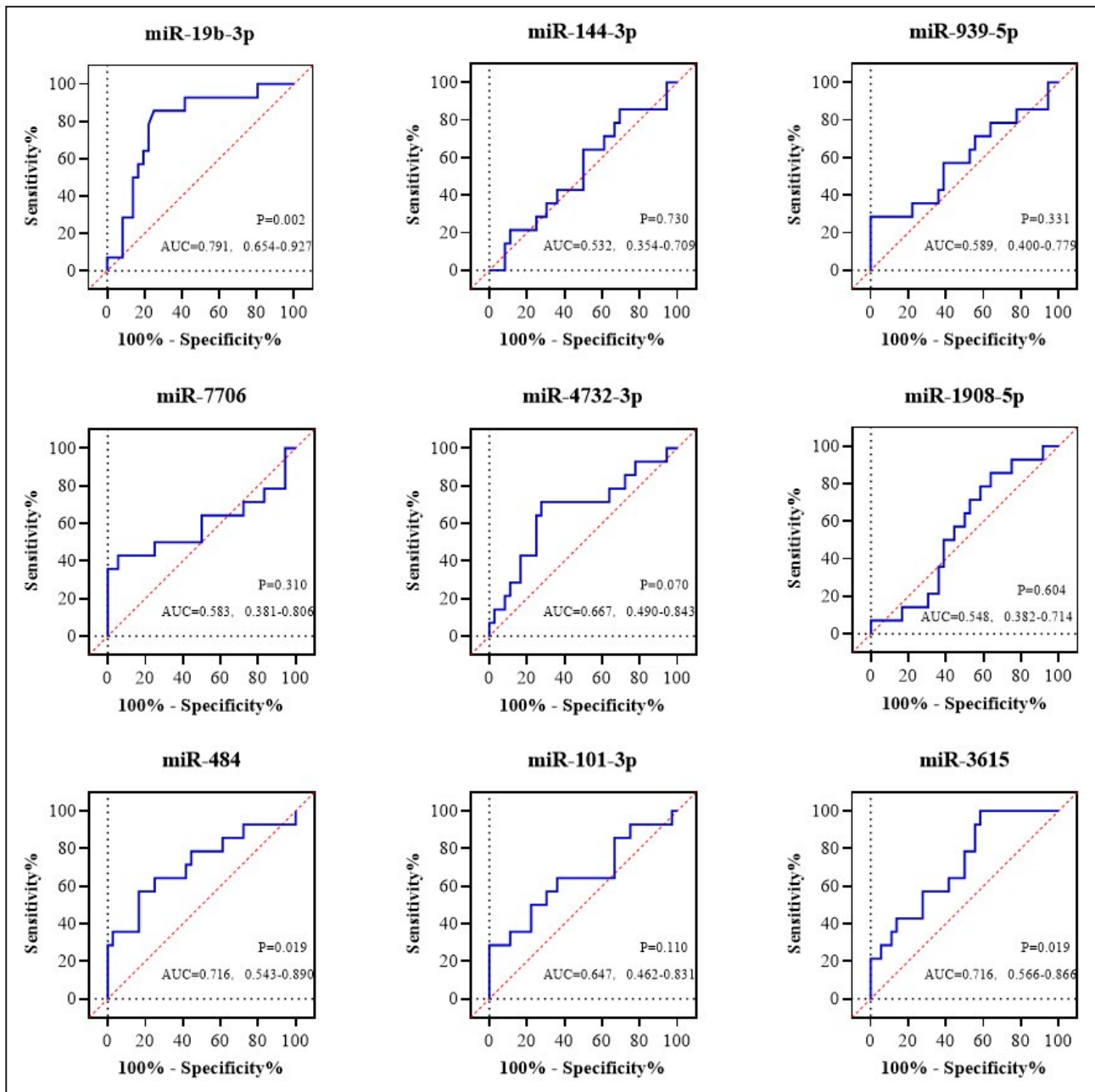


Figure 4. Prognostic power of 9 validated miRNAs by receiver operating characteristic curves.

Receiver operating characteristic curves were performed to test the diagnostic value of 9 miRNA candidates for AHF in PCR-discovery cohort. miR-19b-3p was found to have the highest discriminative potential for AHF (AUC=0.753). AHF denotes acute heart failure, AUC area under curve. Lower right annotation in each figure showed AUC with 95% CI and *P* value.

biomarker for patients with AHF, while the mechanism that aggravating cardiac dysfunction remained to be further investigated.

In addition, HF treatment is another crucial factor that would affect the prognosis. While in our prospective cohort, all of the patients were consecutively enrolled and received standard-of-care in hospital, and discharged with similar regimen across the quartiles (Table S3). Therefore, in our study, the treatment has little impact on outcome.

However from another perspective, studies conducted previously have demonstrated that the level of circulating miRNAs is variable in response to treatment, and the change of miRNAs during admission could also predict adverse outcomes.^{9,25} Thus, it is an important topic to investigate how specific medication interacts with miRNA in the treatment process of HF. Thus, repeated measurement could also be of clinical importance and further studies are warranted.

Table. Clinical Characteristics of 564 Patients With AHF in Quartiles of miR-19b-3p Levels

	Overall (N=564)	Q1 (N=141)	Q2 (N=141)	Q3 (N=141)	Q4 (N=141)	P value
Age, y	69.0 (62.0, 77.0)	70.0 (63.0, 82.0)	68.0 (61.0, 77.0)	69.0 (62.0, 75.0)	70.0 (61.0, 78.0)	0.214
Male/female, n/n	404/160	99/42	99/42	101/40	105/36	0.790
BMI, kg/m ²	24.3±3.6	24.3±3.6	24.0±3.8	24.5±3.6	24.5±3.6	0.950
Smoking, n (%)	175 (31.0)	47 (33.3)	43 (30.5)	49 (34.8)	36 (25.5)	0.456
NYHA functional class	2.4±0.8	2.4±0.8	2.4±0.7	2.3±0.8	2.5±0.8	0.080
HR, bpm	83.7±18.5	83.9±18.7	84.1±17.9	83.7±18.6	82.9±19.0	0.977
SBP, mm Hg	135.5±23.7	137.1±23.3	133.6±23.4	134.5±24.5	137.0±23.7	0.900
DBP, mm Hg	79.2±15.8	79.6±15.5	78.9±15.6	78.7±15.5	79.4±16.6	0.847
Comorbidities						
Diabetes, n (%)	205 (36.4)	45 (31.9)	50 (35.5)	53 (37.6)	57 (40.4)	0.463
Hypertension, n (%)	373 (66.1)	95 (67.4)	81 (57.4)	93 (66.0)	104 (73.8)	0.024*
CHD, n (%)	344 (61.0)	82 (58.2)	85 (60.3)	89 (63.1)	88 (62.4)	0.657
AF, n (%)	118 (20.9)	37 (26.2)	24 (17.0)	31 (22.0)	26 (18.4)	0.205
ICM, n (%)	123 (21.8)	30 (21.3)	30 (21.3)	34 (24.1)	29 (20.6)	0.893
HCM, n (%)	8 (1.4)	2 (1.4)	1 (0.7)	2 (1.4)	3 (2.1)	0.798
DCM, n (%)	31 (5.5)	10 (7.1)	4 (2.8)	8 (5.7)	9 (6.4)	0.418
Serological measurements						
NT-proBNP, ng/mL	1918.0 (782.5, 5070.5)	2170.0 (993.7, 4748.0)	1960.0 (800.6, 5051.3)	1986.0 (609.0, 6771.0)	1636.0 (871.9, 4723.0)	0.261
vmiR-19b-3p (relative expression)	2.15 (1.63, 3.40)	1.23 (0.99, 1.43)	1.89 (1.75, 2.00)	2.69 (2.36, 2.96)	5.24 (4.28, 6.73)	<0.001*
sST2, ng/mL	42.3 (36.8, 50.7)	38.4 (33.0, 42.4)	40.6 (35.4, 47.2)	42.6 (48.4, 38.5)	53.4 (44.9, 67.4)	<0.001*
HDL, mmol/L	0.96 (0.79, 1.20)	1.02 (0.81, 1.31)	0.98 (0.81, 1.25)	0.93 (0.79, 1.13)	0.94 (0.78, 1.15)	0.521
LDL, mmol/L	2.16±0.93	2.07±0.91	2.15±0.98	2.24±0.94	2.19±0.88	0.627
eGFR, mL/(min*1.73 m ²)	79.2 (56.4, 99.3)	82.1 (64.2, 101.7)	81.4 (55.5, 102.9)	79.2 (57.8, 98.0)	73.6 (54.9, 95.7)	0.355
BUN, mmol/L	8.3±6.0	7.7±3.9	8.4±4.5	8.7±9.3	8.5±4.9	0.361
Hb1Ac (%)	6.3 (5.8, 7.4)	6.4 (5.8, 7.3)	6.3 (5.8, 7.5)	6.2 (5.7, 7.0)	6.3 (5.8, 7.5)	0.678
Echocardiographic measurements						
LVEF (%)	43.0 (32.0, 55.0)	44.0 (33.0, 55.0)	43.0 (30.0, 55.0)	44.0 (35.8, 56.0)	40.0 (32.3, 54.8)	0.675
IVST, mm	10.0 (9.0, 11.0)	9.0 (9.0, 10.0)	9.0 (9.0, 10.0)	10.0 (9.0, 10.0)	11.0 (10.0, 13.0)	<0.001*
LVPWT, mm	10.0 (9.0, 10.0)	10.0 (9.0, 10.0)	10.0 (9.0, 10.0)	10.0 (9.0, 10.0)	10.0 (9.0, 11.0)	0.001*
LVeDD, mm	50.0 (45.0, 57.0)	49.0 (44.0, 56.0)	50.0 (44.0, 57.0)	49.0 (45.0, 56.0)	51.0 (45.0, 60.0)	0.151
LVeSD, mm	35.5 (30.0, 46.0)	32.0 (29.0, 43.0)	31.0 (27.0, 45.0)	34.0 (28.0, 44.0)	37.0 (30.0, 47.0)	0.241
LVMi, g/m ²	113.5±34.8	101.0±28.1	103.8±25.2	110.2±26.8	141.1±42.2	<0.001*

Continuous variables are presented as means±SD if conform normal distribution or median with interquartile range (IQR) if not. Categorical variables are presented as percentage (%). AF indicates atrial fibrillation; AHF, acute heart failure; BMI, body mass index; BUN, blood urea nitrogen; CHD, coronary heart disease; DBP, diastolic blood pressure; DCM, dilated cardiomyopathy; eGFR, estimated glomerular filtration rate (calculated by MDRD formula); Hb1Ac, hemoglobin A1c; HCM, hypertrophic cardiomyopathy; HDL, high-density lipoprotein; HR, heart rate; ICM, ischemic cardiomyopathy; IVST, interventricular septum thickness; LDL, low-density lipoprotein; LVeDD, left ventricular end-diastolic diameter; LVEF, left-ventricular ejection fraction; LVeSD, left ventricular end-systolic diameter; LVMi, left ventricular mass index; LVPWT, left ventricular posterior wall thickness; NT-proBNP, N-terminal brain natriuretic peptide precursor; NYHA, New York Heart Association; SBP, systolic blood pressure; and sST2, soluble suppression of tumorigenicity 2.

*Significant P value (<0.05).

Limitations

The present study has several limitations. First, although the other 8 miRNAs failed to outperform miR-19b-3p, they could potentially also play a role in diagnosis and prognostication of patients with HF. Combining evaluation with diverse miRNAs, NT-proBNP, or other valuable markers could be considered in further investigations.

Second, we did not repetitively measure the level of miR-19b-3p during admission and follow-up. As miRNAs are dynamic, further studies analyzing repetitive measurement of miR-19b-3p are warranted to explore further clinical implication. Third, echocardiography and serum sST2 were not designed to be measured during follow-up, thus it remained unknown whether miR-19b-3p level correlates with follow-up changes

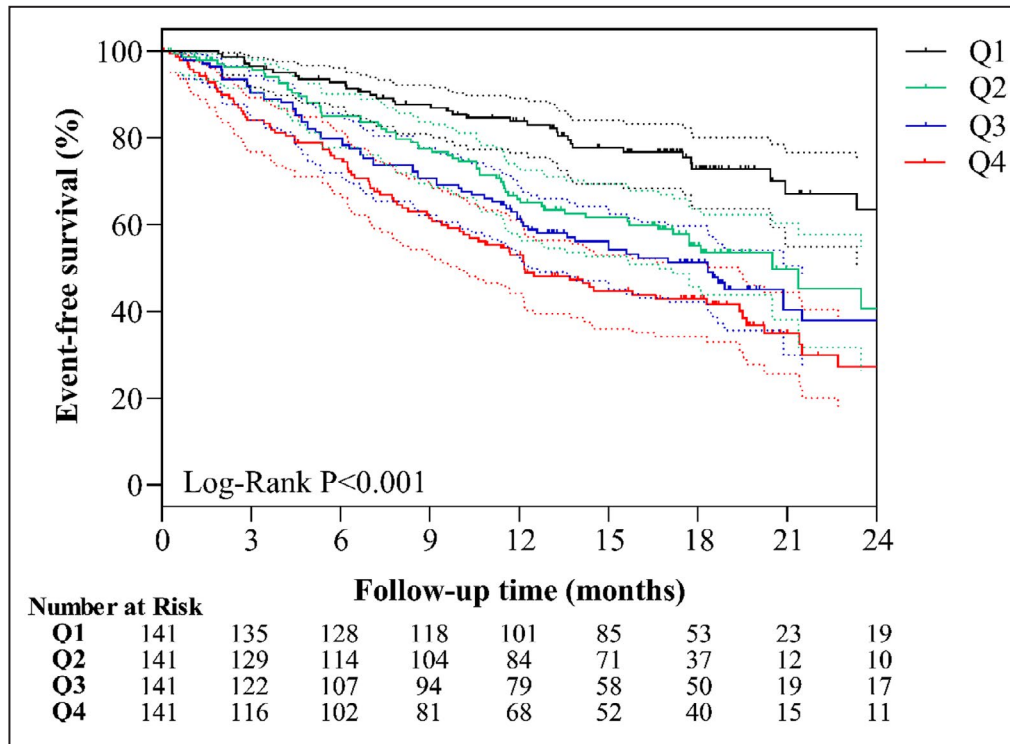


Figure 5. Survival analysis of patients with AHF divided by baseline level of miR-19b-3p. Survival analysis of miR-19b-3p for primary end point (all-cause mortality or readmission due to HF) were performed and survival curves with 95% CI shown with dotted line in corresponding color. Through a follow-up period of 19.1 [17.7, 20.7] months, survival curves showed group with higher level of miR-19b-3p presented worse event-free survival, with Log-Rank *P* value <0.001. Q1, Q2, Q3 and Q4 represent patients with AHF with relative expression of miR-19b-3p level lower than 1.63, 1.63-2.15, 2.15-3.41, and higher than 3.41, respectively.

of echocardiographic indices and serum biomarkers. Fourth, we evaluated only ventricular structural parameters by echocardiography, which are not the gold standard for measuring the extent and character of cardiac hypertrophy. Further extensive studies using cardiac magnetic resonance are needed to support the findings. Fifth, in the screening and PCR discovery

phase, we performed only ROC analysis without k-fold cross validation of AUCs. K-fold analysis is an advantageous approach that could reduce the generalization error and produce a more precise result. However, in our study, the discovery cohort had a limited sample size that was inadequate and independent of a validation cohort, rendering it inappropriate to perform k-fold

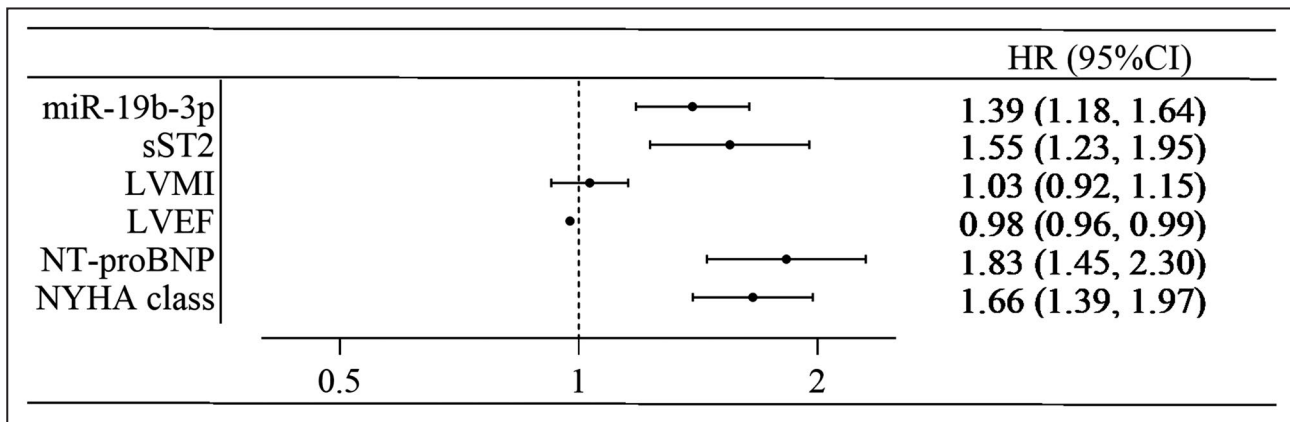


Figure 6. The Forest plot of multivariate Cox proportional hazard regression model for prognostic evaluation. The level of miR-19b-3p, sST2, and NT-proBNP was analyzed after logarithmic transformation.

analysis. Further studies with a larger sample size are warranted.

CONCLUSIONS

Circulating miR-19b-3p is independently associated with adverse clinical outcomes in patients with AHF. In addition, a high level of circulating miR-19b-3p might indicate adverse cardiac hypertrophy in AHF. Further studies are warranted to reveal the regulatory mechanism underlying the increase in miR-19b-3p during AHF.

ARTICLE INFORMATION

Received May 14, 2021; accepted August 19, 2021.

Affiliations

Department of Cardiology, Shanghai Tenth People's Hospital, Tongji University School of Medicine, Shanghai, China (Y.S., Y.S., Y.T., H.L., X.W., X.P., W.L., X.Z., Y.X., D.X.); Department of Cardiology, Qidong People's Hospital, Qidong, Jiangsu, China (Y.S., F.Z., C.Y., D.X.); Centre for Cardiovascular Genomics and Medicine (CCGM), Lui Che Woo Institute of Innovative Medicine, Chinese University of Hong Kong (CUHK), Hong Kong SAR (S.O.); Department of Medicine and Therapeutics, Faculty of Medicine, CUHK, Hong Kong SAR (S.O.); Hong Kong Hub of Paediatric Excellence (HK HOPE), Hong Kong Children's Hospital (HKCH), Kowloon Bay, Hong Kong SAR (S.O.); Institute for Translational Medicine, Xiamen Cardiovascular Hospital, Xiamen University, Xiamen, Fujian, China (S.O.); and Kunming Institute of Zoology - The Chinese University of Hong Kong (KIZ-CUHK), Joint Laboratory of Bioresources and Molecular Research of Common Diseases, Kunming Institute of Zoology, Chinese Academy of Sciences, Kunming, Yunnan, China (S.O.).

Acknowledgments

We gratefully acknowledge the support from the Heart Failure Project Team of the Department of Cardiology, Shanghai Tenth People's Hospital, Tongji University School of Medicine, Shanghai, China.

Sources of Funding

This work has been supported by grants from National Natural Science Foundation of China (No. 81770391 to Dachun Xu) and Clinical Research Plan of Shanghai Hospital Development Center (No. SHDC2020CR3030B to Dachun Xu). Sang-Bing Ong is supported by a Direct Grant for Research 2020/21 (2020.035), a Project Impact Enhancement Fund (PIEF) (Phase 2-COVID) (PIEF/Ph2/COVID/08), the Improvement on Competitiveness in Hiring New Faculties Funding Scheme from the Chinese University of Hong Kong (CUHK) and the Lui Che Woo Foundation.

Disclosures

None.

Supplementary Material

Data S1
Tables S1–S3
Figures S1–S2

REFERENCES

- Ponikowski P, Voors AA, Anker SD, Bueno H, Cleland JG, Coats AJ, Falk V, Gonzalez-Juanatey JR, Harjola VP, Jankowska EA, et al. 2016 ESC guidelines for the diagnosis and treatment of acute and chronic heart failure: the task force for the diagnosis and treatment of acute and chronic heart failure of the European Society of Cardiology (ESC). Developed with the special contribution of the Heart Failure Association (HFA) of the ESC. *Eur J Heart Fail.* 2016;18:891–975. doi: 10.1093/eurheartj/ehw128
- Vegter EL, van der Meer P, de Windt LJ, Pinto YM, Voors AA. MicroRNAs in heart failure: from biomarker to target for therapy. *Eur J Heart Fail.* 2016;18:457–468. doi: 10.1002/ehfj.495
- Gomes CPC, Schroen B, Kuster GM, Robinson EL, Ford K, Squire IB, Heymans S, Martelli F, Emanuelli C, Devaux Y, et al. Regulatory RNAs in heart failure. *Circulation.* 2020;141:313–328. doi: 10.1161/CIRCULATIONAHA.119.042474
- Vogel B, Keller A, Frese KS, Leidinger P, Sedaghat-Hamedani F, Kayvanpour E, Kloos W, Backe C, Thanaraj A, Brefort T, et al. Multivariate miRNA signatures as biomarkers for non-ischaemic systolic heart failure. *Eur Heart J.* 2013;34:2812–2822. doi: 10.1093/eurheartj/ehs256
- Gupta SK, Foinquinos A, Thum S, Remke J, Zimmer K, Bauters C, de Groote P, Boon RA, de Windt LJ, Preissl S, et al. Preclinical development of a microRNA-based therapy for elderly patients with myocardial infarction. *J Am Coll Cardiol.* 2016;68:1557–1571. doi: 10.1016/j.jacc.2016.07.739
- Goren Y, Kushnir M, Zafrir B, Tabak S, Lewis BS, Amir O. Serum levels of microRNAs in patients with heart failure. *Eur J Heart Fail.* 2012;14:147–154. doi: 10.1093/eurjhf/hfr155
- Wong LL, Zou R, Zhou L, Lim JY, Phua DCY, Liu C, Chong JPC, Ng JYX, Liew OW, Chan SP, et al. Combining circulating microRNA and NT-proBNP to detect and categorize heart failure subtypes. *J Am Coll Cardiol.* 2019;73:1300–1313. doi: 10.1016/j.jacc.2018.11.060
- Zhu X, Wang H, Liu F, Chen L, Luo W, Su P, Li W, Yu L, Yang X, Cai J. Identification of micro-RNA networks in end-stage heart failure because of dilated cardiomyopathy. *J Cell Mol Med.* 2013;17:1173–1187. doi: 10.1111/jcmm.12096
- Ovchinnikova ES, Schmitter D, Vegter EL, ter Maaten JM, Valente MAE, Liu LCY, van der Harst P, Pinto YM, de Boer RA, Meyer S, et al. Signature of circulating microRNAs in patients with acute heart failure. *Eur J Heart Fail.* 2016;18:414–423. doi: 10.1002/ehfj.332
- Gurha P, Abreu-Goodger C, Wang T, Ramirez MO, Drummond AL, van Dongen S, Chen Y, Bartonicek N, Enright AJ, Lee B, et al. Targeted deletion of microRNA-22 promotes stress-induced cardiac dilation and contractile dysfunction. *Circulation.* 2012;125:2751–2761. doi: 10.1161/CIRCULATIONAHA.111.044354
- Gaede L, Liebetrau C, Blumenstein J, Troidl C, Dorr O, Kim WK, Gottfried K, Voss S, Berkowitsch A, Walther T, et al. Plasma microRNA-21 for the early prediction of acute kidney injury in patients undergoing major cardiac surgery. *Nephrol Dial Transplant.* 2016;31:760–766. doi: 10.1093/ndt/gfw007
- Sun SQ, Zhang T, Ding D, Zhang WF, Wang XL, Sun Z, Hu LH, Qin SY, Shen LH, He B. Circulating microRNA-188, -30a, and -30e as early biomarkers for contrast-induced acute kidney injury. *J Am Heart Assoc.* 2016;5:e004138. doi: 10.1161/JAHA.116.004138
- Lang RM, Bierig M, Devereux RB, Flachskampf FA, Foster E, Pellikka PA, Picard MH, Roman MJ, Seward J, Shanewise JS, et al. Recommendations for chamber quantification: a report from the American Society of Echocardiography's guidelines and standards committee and the chamber quantification writing group, developed in conjunction with the European Association of Echocardiography, a branch of the European Society of Cardiology. *J Am Soc Echocardiogr.* 2005;18:1440–1463. doi: 10.1016/j.echo.2005.10.005
- Xiao J, Gao R, Bei Y, Zhou Q, Zhou Y, Zhang H, Jin M, Wei S, Wang K, Xu X, et al. Circulating miR-30d predicts survival in patients with acute heart failure. *Cell Physiol Biochem.* 2017;41:865–874. doi: 10.1159/000459899
- Weir RA, Miller AM, Murphy GE, Clements S, Steedman T, Connell JM, McInnes IB, Dargie HJ, McMurray JJ. Serum soluble ST2: a potential novel mediator in left ventricular and infarct remodeling after myocardial infarction. *J Am Coll Cardiol.* 2010;55:243–250. doi: 10.1016/j.jacc.2009.08.047
- Nachamkin I, Panaro NJ, Li M, Ung H, Yuen PK, Kricka LJ, Wilding P. Agilent 2100 bioanalyzer for restriction fragment length polymorphism analysis of the campylobacter jejuni flagellin gene. *J Clin Microbiol.* 2001;39:754–757. doi: 10.1128/JCM.39.2.754-757.2001
- Nair SS, Luu PL, Qu W, Maddugoda M, Huschtscha L, Reddel R, Chenex-Trench G, Toso M, Kench JG, Horvath LG, et al. Guidelines for whole genome bisulphite sequencing of intact and FFPET DNA on the illumina HiSeq X Ten. *Epigenetics Chromatin.* 2018;11:24. doi: 10.1186/s13072-018-0194-0
- de Ronde MWJ, Ruijter JM, Lanfear D, Bayes-Genis A, Kok MGM, Creemers EE, Pinto YM, Pinto-Sietsma SJ. Practical data handling

- pipeline improves performance of qPCR-based circulating miRNA measurements. *RNA*. 2017;23:811–821. doi: 10.1261/rna.059063.116
19. Livak KJ, Schmittgen TD. Analysis of relative gene expression data using real-time quantitative PCR and the $2^{-\Delta\Delta C(T)}$ method. *Methods*. 2001;25:402–408. doi: 10.1006/meth.2001.1262
 20. Yusuf NH, Ong WD, Redwan RM, Latip MA, Kumar SV. Discovery of precursor and mature microRNAs and their putative gene targets using high-throughput sequencing in pineapple (*Ananas comosus* var. *comosus*). *Gene*. 2015;571:71–80. doi: 10.1016/j.gene.2015.06.050
 21. Griffiths-Jones S, Saini HK, van Dongen S, Enright AJ. Mirbase: tools for microRNA genomics. *Nucleic Acids Res*. 2008;36:D154–D158.
 22. Anders S, Huber W. Differential expression analysis for sequence count data. *Genome Biol*. 2010;11:R106.
 23. John B, Enright AJ, Aravin A, Tuschl T, Sander C, Marks DS. Human microRNA targets. *PLoS Biol*. 2004;2:e363. doi: 10.1371/journal.pbio.0020363
 24. Scrutinio D, Conserva F, Passantino A, Iacoviello M, Lagioia R, Gesualdo L. Circulating microRNA-150-5p as a novel biomarker for advanced heart failure: a genome-wide prospective study. *J Heart Lung Transplant*. 2017;36:616–624. doi: 10.1016/j.healun.2017.02.008
 25. van Boven N, Kardys I, van Vark LC, Akkerhuis KM, de Ronde MWJ, Khan MAF, Merkus D, Liu Z, Voors AA, Asselbergs FW, et al. Serially measured circulating microRNAs and adverse clinical outcomes in patients with acute heart failure. *Eur J Heart Fail*. 2018;20:89–96. doi: 10.1002/ejhf.950
 26. Wu T, Chen Y, Du Y, Tao J, Li W, Zhou Z, Yang Z. Circulating exosomal miR-92b-5p is a promising diagnostic biomarker of heart failure with reduced ejection fraction patients hospitalized for acute heart failure. *J Thorac Dis*. 2018;10:6211–6220. doi: 10.21037/jtd.2018.10.52
 27. Li G, Song Y, Li YD, Jie LJ, Wu WY, Li JZ, Zhang Q, Wang Y. Circulating miRNA-302 family members as potential biomarkers for the diagnosis of acute heart failure. *Biomark Med*. 2018;12:871–880. doi: 10.2217/bmm-2018-0132
 28. Corsten MF, Dennert R, Jochems S, Kuznetsova T, Devaux Y, Hofstra L, Wagner DR, Staessen JA, Heymans S, Schroen B. Circulating microRNA-208b and microRNA-499 reflect myocardial damage in cardiovascular disease. *Circ Cardiovasc Genet*. 2010;3:499–506. doi: 10.1161/CIRCGENETICS.110.957415
 29. Danielson LS, Park DS, Rotllan N, Chamorro-Jorganes A, Guizarro MV, Fernandez-Hernando C, Fishman GI, Phoon CK, Hernando E. Cardiovascular dysregulation of miR-17-92 causes a lethal hypertrophic cardiomyopathy and arrhythmogenesis. *FASEB J*. 2013;27:1460–1467. doi: 10.1096/fj.12-221994
 30. Zou M, Wang F, Gao R, Wu J, Ou Y, Chen X, Wang T, Zhou X, Zhu W, Li P, et al. Autophagy inhibition of hsa-miR-19a-3p/19b-3p by targeting TGF-beta R II during TGF-beta1-induced fibrogenesis in human cardiac fibroblasts. *Sci Rep*. 2016;6:24747. doi: 10.1038/srep24747
 31. Zhong C, Wang K, Liu Y, Lv D, Zheng BO, Zhou Q, Sun QI, Chen P, Ding S, Xu Y, et al. miR-19b controls cardiac fibroblast proliferation and migration. *J Cell Mol Med*. 2016;20:1191–1197. doi: 10.1111/jcmm.12858
 32. Bayes-Genis A, de Antonio M, Vila J, Penafiel J, Galan A, Barallat J, Zamora E, Urrutia A, Lupon J. Head-to-head comparison of 2 myocardial fibrosis biomarkers for long-term heart failure risk stratification: ST2 versus galectin-3. *J Am Coll Cardiol*. 2014;63:158–166. doi: 10.1016/j.jacc.2013.07.087
 33. Sygitowicz G, Tomaniak M, Filipiak KJ, Koltowski L, Sitkiewicz D. Galectin-3 in patients with acute heart failure: preliminary report on first polish experience. *Adv Clin Exp Med*. 2016;25:617–623. doi: 10.17219/acem/60527
 34. Fang L, Ellims AH, Moore XL, White DA, Taylor AJ, Chin-Dusting J, Dart AM. Circulating microRNAs as biomarkers for diffuse myocardial fibrosis in patients with hypertrophic cardiomyopathy. *J Transl Med*. 2015;13:314. doi: 10.1186/s12967-015-0672-0
 35. Gawor M, Spiewak M, Kubik A, Wrobel A, Lutynska A, Marczak M, Grzybowski J. Circulating biomarkers of hypertrophy and fibrosis in patients with hypertrophic cardiomyopathy assessed by cardiac magnetic resonance. *Biomarkers*. 2018;23:676–682. doi: 10.1080/1354750X.2018.1474261
 36. Copier CU, Leon L, Fernandez M, Contador D, Calligaris SD. Circulating miR-19b and miR-181b are potential biomarkers for diabetic cardiomyopathy. *Sci Rep*. 2017;7:13514.
 37. Wang WB, Li HP, Yan J, Zhuang F, Bao M, Liu JT, Qi YX, Han Y. CTGF regulates cyclic stretch-induced vascular smooth muscle cell proliferation via microRNA-19b-3p. *Exp Cell Res*. 2019;376:77–85.
 38. Mehta JL, Mercanti F, Stone A, Wang X, Ding Z, Romeo F, Khaidakov M. Gene and microRNA transcriptional signatures of angiotensin II in endothelial cells. *J Cardiovasc Pharmacol*. 2015;65:123–129. doi: 10.1097/FJC.0000000000000118
 39. Chen W, Zhou ZQ, Ren YQ, Zhang L, Sun LN, Man YL, Wang ZK. Effects of long non-coding RNA LINC00667 on renal tubular epithelial cell proliferation, apoptosis and renal fibrosis via the miR-19b-3p/LINC00667/CTGF signaling pathway in chronic renal failure. *Cell Signal*. 2019;54:102–114. doi: 10.1016/j.cellsig.2018.10.016

SUPPLEMENTAL MATERIAL

Data S1.

Supplemental Methods

miRNA expression profiling

RNA extraction and small RNA sequencing

Total RNA was extracted from serum samples using the Qiagen miRNeasy Serum/Plasma Kit (cat. No. 217184, QIAGEN, Germany) according to the manufacturer's protocol. Quantitation of total RNA was carried out using the Nanodrop 2000 (Thermo Fisher Scientific Inc., USA). RNA integrity was assessed by Agilent 2100 Bioanalyzer (Agilent Technology, USA).¹⁶ 1 µg total RNA of each sample was used for the small RNA library construction using TruSeq Small RNA Sample Prep Kits (Cat. No. RS-200-0012, Illumina, USA). The libraries were finally sequenced using the Illumina HiSeq X Ten platform and 150 bp paired-end reads were generated.¹⁷

Confirmation and validation of miRNA by RT-qPCR in PCR-discovery and validation cohorts.

Quantification of miRNAs was performed via two stepwise processes: reverse transcription and polymerase chain reaction (PCR). First, total RNA extracted was reverse transcribed using the miRNA 1st Strand cDNA Synthesis Kit (cat. No. AT351, TransGene Biotech Inc., China). Real-time PCR was performed using LightCycler® 480 II Real-time PCR Instrument (Roche, Swiss) with 10 µL PCR reaction mixture that included 1 µL of cDNA, 5 µL of 2×PerfectStart™ Green qPCR SuperMix (cat. No.

AQ601, TransGene, China), 0.2 μ L of universal primer, 0.2 μ L of miRNA-specific primer and 3.6 μ L of nuclease-free water. Each sample was run in triplicate for analysis.¹⁸ The miRNA-specific primer sequences were designed based on the miRNA sequences (primers were exhibited below). The expression levels of miRNAs were normalized to 5S rRNA and were calculated using the $2^{-\Delta\Delta C_t}$ method.¹⁹

Bioinformatics analysis of RNA-sequence data

The raw data generated by Illumina sequencing were analyzed as previously described.²⁰ The known miRNAs were identified by aligning against miRBase v22 database (<http://www.mirbase.org/>)²¹, and the miRNA expression was calculated by transcript per million (TPM, the number of reads per miRNA matched/all reads $\times 1 \times 10^6$). Differentially expressed miRNAs were calculated and filtered with the threshold of P value < 0.05 and absolute \log_2 (fold change) > 1 using DESeq R package²² (version 1.18.0). The targets of differentially expressed miRNAs were predicted by miRanda software²³ with parameters as follows: $S \geq 150$, $\Delta G \leq -30$ kcal/mol and demand strict 5' seed pairing. GO enrichment and KEGG pathway enrichment analysis of DEM-target-Genes were respectively performed using R based on the hypergeometric distribution.

Table S1. Primer sequences of 40 miRNAs.

ID	Primer sequences (5'-3')
miR-19b-3p	TGTGCAAATCCATGCAAAACTGA
miR-4732-3p	CCTGACCTGTCCTGTTCTG
miR-205-5p	TTCCTTCATTCCACCGGAGTCTG
miR-16-2-3p	CGCGCCAATATTACTGTGCTGCTTTA
miR-15b-5p	CGCTAGCAGCACATCATGGTTTACA
miR-148b-3p	TATCCTGCCCCGAGCTGAGC
miR-3615	CTCGGCTCCTCGCGGCTC
miR-2110	TATTGGGGAAACGGCCGCT
miR-3940-3p	ATATATACAGCCCGGATCCCAGCC
miR-142-5p	GCGCGCATAAAGTAGAAAGCACTACT
miR-143-3p	CGCTGAGATGAAGCACTGTAGCTC
miR-4685-3p	TCTCCCTTCCTGCCCTGG
miR-885-5p	CCTCCATTACACTACCCTGCCTCT
miR-1180-3p	TATATATTTCCGGCTCGCGTGGGT
miR-484	GGCTCAGTCCCCTCCCGAT
miR-424-3p	CCAAAACGTGAGGCGCTGCTAT
miR-1292-5p	TATATATGGGAACGGGTTCCGGCA
let-7b-3p	CGCTATAACAACCTACTGCCTTCCC
miR-4732-5p	GCCCTGACCTGTCCTGTTCT
miR-103a-3p	CAGCAGCATTGTACAGGGCTATGA
miR-204-5p	CGTTCCCTTTGTTCATCCTATGCCT
miR-200c-3p	GCGTAATACTGCCGGGTAATGATGGA
miR-144-3p	GCGCTACAGTATAGATGATGT
miR-100-5p	CCAACCCGTAGATCCGAACCTTGTG
miR-24-3p	TGGCTCAGTTCAGCAGGAACAG
miR-183-5p	TCGCTATGGCACTGGTAGAATTCCT
miR-21-5p	CGCCGTAGCTTATCAGACTGATGTTGA
miR-939-5p	TGGGGAGCTGAGGCTCTG
miR-223-3p	CGCTGTCAGTTTGTCAAATACCCCA
let-7c-5p	CGCCTGAGGTAGTAGGTTGTATGGTT
miR-1908-5p	CGGGGACGGCGATTGGTC
miR-605-3p	CCGCGAGAAGGCACTATGAGATTTAGA
miR-365a/b-3p	GCGCGTAATGCCCTAAAATCCTTAT
let-7e-5p	CGCGTGAGGTAGGAGGTTGTATAGTT
miR-199a/b-3p	CGCACAGTAGTCTGCACATTGGTTA
miR-7706	CGCCTGTGCTCTGCCGAGA
miR-1271-5p	CTTGGCACCTAGCAAGCACTCA
miR-101-3p	CGCTACAGTACTGTGATAACTG
miR-17-5p	GCCAAAGTGCTTACAGTGCAGGTAG
miR-664a-3p	CCGCTATTCATTTATCCCCAGCCTACA

Table S2. Patient characteristics of screening and PCR-discovery cohorts.

	Screening cohort			PCR-discovery cohort		
	control (N=5)	AHF (N=15)	P-value	control (N=26)	AHF (N=50)	P-value
Age (years)	58.2±7.7	65.7±10.2	0.115	62.4±10.6	67.8±11.1	0.948
Male/female (n/n)	1/4	9/6	0.303	10/16	13/37	0.262
Current smoking, n (%)	0 (0)	6 (40)	0.260	4 (15.38)	13 (26.00)	0.292
LVEF (%)	65.4±2.6	28.7±7.9	<0.001*	63.0 (62.0-64.5)	42.0 (30.5-60.0)	0.001*
NYHA functional class	n.a.	2.93±0.26	n.a.	n.a.	2.60±0.64	n.a.
HF history, n (%)	0 (0)	9 (60)	0.038*	4(15.38)	13(26.00)	0.292
NT-proBNP (ng/L)	78 (55-110)	2521 (634-7867)	<0.001*	40.6 (24.3-108.0)	1281.0 (733.0-3380.0)	<0.001*
SBP (mmHg)	127.4±21.6	129.3±26.5	0.874	142.2±25.0	131.9±21.0	0.135
DBP (mmHg)	76.6±10.4	72.8±17.4	0.568	75.8±22.9	79.5±14.1	0.589
DM, n (%)	0 (0)	5 (33.3)	0.266	4 (15.38)	18 (36.00)	0.060
HTN, n (%)	1 (20)	7 (46.7)	0.603	8 (30.77)	22 (44.00)	0.263
HDL (mmol/L)	1.71±0.33	1.02±0.32	0.004*	1.19 (0.98-1.37)	0.87 (0.78-1.24)	0.044*
LDL (mmol/L)	2.73±0.69	2.05±1.17	0.235	2.61±1.15	2.30±0.93	0.104
ALT (IU/L)	29.4±18.1	37.4±25.4	0.461	27.6±19.2	36.8±41.3	0.768
WBC (/nL)	6.6±1.0	7.1±1.8	0.480	6.72 (5.18-7.25)	6.64 (5.43-8.53)	0.517
HB (g/L)	121.0±9.4	135.1±21.3	0.058	130.4±10.4	127.1±23.5	0.062
CRP (mg/L)	3.02 (2.34-3.23)	3.13 (3.02-8.41)	0.343	3.02(2.25-3.75)	8.24(2.43-17.64)	0.058
eGFR (mL/(min*1.73m ²))	107.7±22.5	76.4±24.4	0.021*	99.6±20.8	74.1±29.3	0.009*
BUN (mmol/L)	6.53±1.44	8.69±7.18	0.287	5.35±1.83	8.57±5.36	0.004*

Continuous variables are presented as means±SD if conform normal distribution or median with interquartile range (IQR) if not. Categorical variables are presented as percentage (%).

* Significant P value (<0.05).

AHF, acute heart failure; LVEF, left-ventricular ejection fraction; NYHA, New York Heart Association; HF, heart failure; NT-proBNP, N-terminal brain natriuretic peptide precursor; SBP, systolic blood pressure; DBP, diastolic blood pressure; DM, diabetes mellitus; HTN, hypertension; HDL, high-density lipoprotein; LDL, low-density lipoprotein; ALT, alanine aminotransferase; WBC, white blood cell count; HB, hemoglobin; CRP, C-reactive protein; eGFR, estimated glomerular filtration rate (calculated by MDRD formula); BUN, blood urea nitrogen; n.a., not applicable.

Table S3. Medication at discharge of the validation cohort.

	Overall (N=564)	Q1 (N=141)	Q2 (N=141)	Q3 (N=141)	Q4 (N=141)	P-value
β-blockers, n (%)	319 (56.6)	76 (53.9)	79 (56.1)	80 (56.7)	84 (59.6)	0.815
ACEIs, n (%)	95 (16.8)	26 (18.4)	24 (17.1)	21 (14.9)	24 (17.1)	0.886
ARBs, n (%)	404 (71.6)	109 (77.3)	95 (67.4)	98 (69.3)	102 (72.3)	0.279
ARNI, n (%)	73 (12.9)	16 (11.3)	19 (13.5)	17 (12.1)	21 (14.9)	0.819
MRAs, n (%)	356 (63.1)	87 (61.7)	90 (63.5)	90 (64.1)	89 (63.0)	0.980
Diuretics, n (%)	131 (23.2)	35 (24.8)	29 (20.6)	29 (20.6)	38 (27.0)	0.803
CCBs, n (%)	208 (36.9)	56 (39.7)	45 (31.9)	49 (34.8)	58 (41.1)	0.341
Nitrates, n (%)	97 (17.2)	24 (17.0)	23 (16.4)	24 (16.9)	23 (16.5)	0.997
Digoxin, n (%)	51 (9.0)	9 (6.4)	11 (7.8)	14 (9.9)	17 (12.1)	0.366
Statins, n (%)	368 (65.2)	91 (64.5)	85 (60.3)	97 (68.8)	95 (67.4)	0.453
Anticoagulants and antiplatelets, n (%)	391 (69.3)	102 (72.3)	89 (63.1)	93 (66.0)	107 (75.9)	0.080

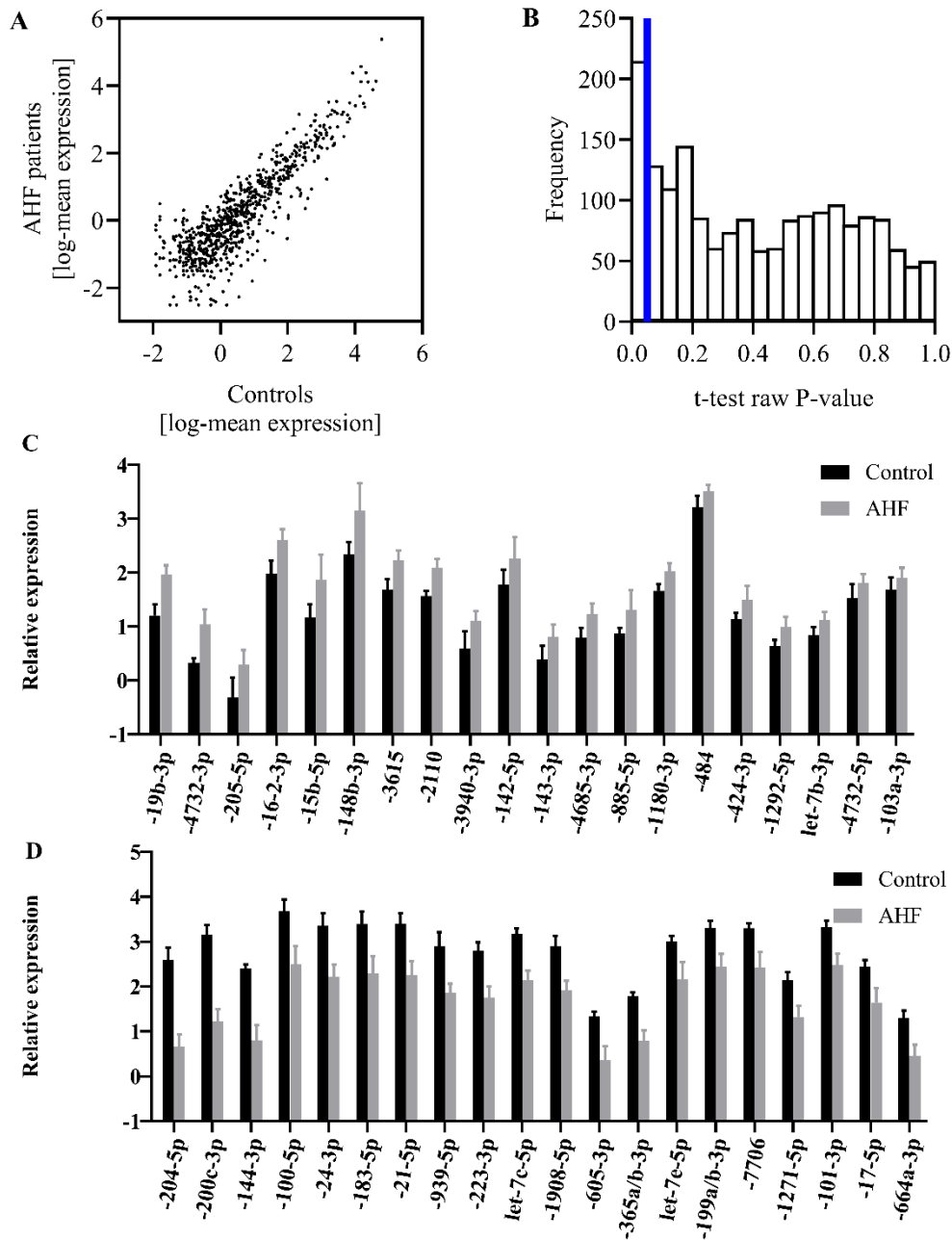
Medication condition is described as categorical variable according to whether specific medicine was taken.

* Significant p value (<0.05).

ACEIs, angiotensin-converting enzyme inhibitors; ARBs, angiotensin receptor blockers; MRAs, mineralocorticoid receptor antagonists; ARNI, angiotensin receptor enkephalin inhibitor; CCBs, calcium-channel blockers.

Figure S1. miRNA screening by RNA-sequencing and PCR discovery of 40 miRNAs

candidates.



A, Matrix plot showed a positive linear correlation of the mean expression between 15 AHF

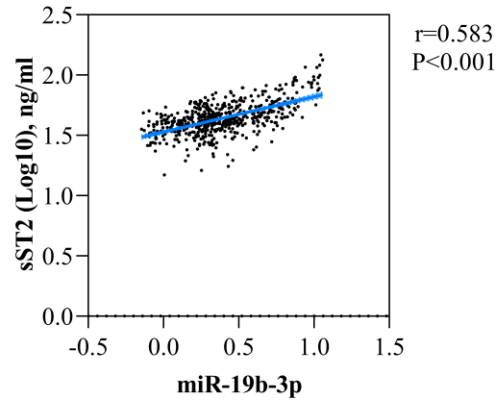
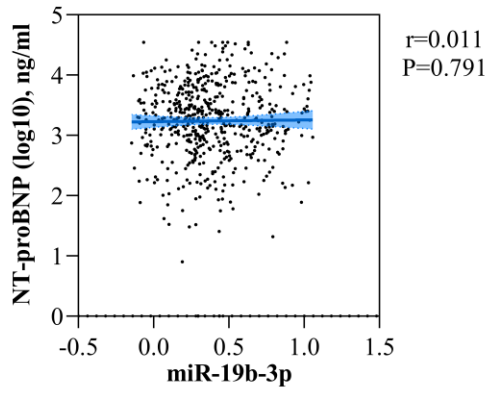
patients and 5 controls. **B**, the histogram of presented the distribution of raw P-values of screened

miRNAs. The blue vertical line draws the boundary of P value=0.05. The bar on the left indicates

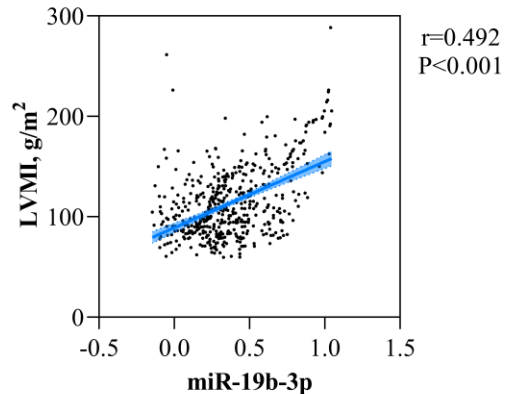
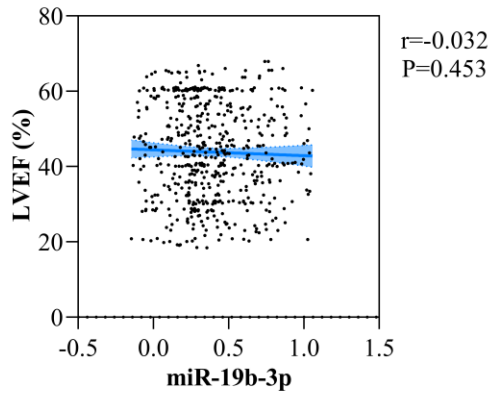
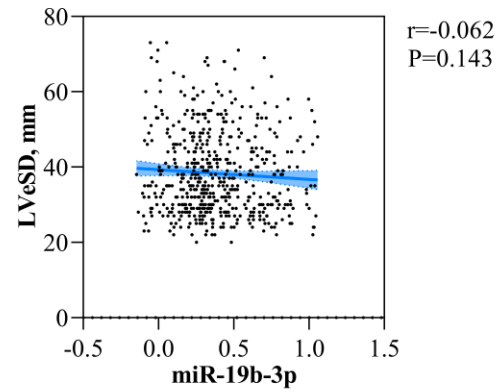
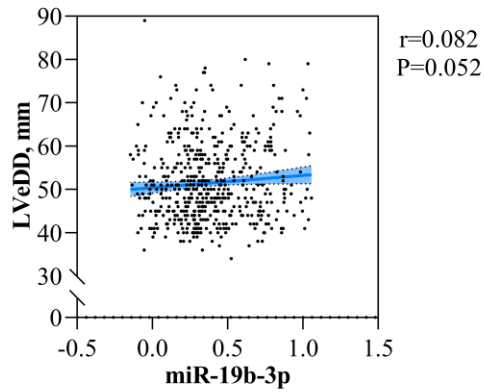
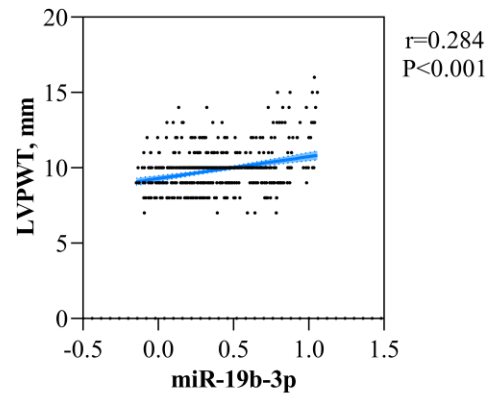
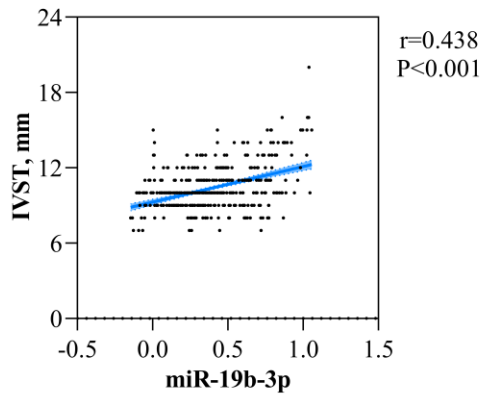
218 differential expressed miRNAs. **1C & 1D** show 20 Up-regulated and 20 down-regulated miRNAs with the highest absolute fold change from the PCR-discovery cohort. Mean relative expression value were normalized to the corresponding values of control subjects and expressed after logarithmic transformation. miRNAs expression levels were calculated by transcript per million. $TPM=N/M*10^6$, N represents reads count for each miRNA, and M represents total reads count of sample. AHF denotes acute heart failure.

Figure S2. Correlations of miR-19b-3p with serological and echocardiographic measurements.

Serological measurements



Echocardiographic measurements



Spearman correlation analysis showed relative expression level of miR-19b-3p significantly positively correlated with sST2, IVST, LVPWT, LVeDD, LVMI, but not NT-proBNP, LVeSD and left ventricular ejection fraction. The levels of NT-proBNP and sST2 were logarithmic transformed. NT-proBNP denotes N-terminal pro brain natriuretic peptide, sST2 soluble suppression of tumorigenicity 2, IVST interventricular septum thickness, LVeDD left ventricular end-diastolic diameter, LVeSD left ventricular end-systolic diameter, LVMI left ventricular mass index, LVPWT left ventricular posterior wall thickness. The light blue area represents 95% confidence interval of correlation coefficient.